Homodyne Detector Characterization

John Stearns, Student
Ryan DeRosa, Mentor

September 23, 2015

Abstract

Currently, Advanced LIGO makes use of a DC readout scheme, a type of homodyne detection in which the light containing the gravitational wave signal is sensed against a local oscillator field generated by a static differential arm length. An alternative scheme is balanced homodyne detection, in which an external local oscillator is combined with the signal beam on a beamsplitter at the dark port. Both outputs are detected and subtracted to yield the gravitational wave readout. This scheme has several advantages, including common mode noise cancellation and facilitating the measurement of sub-quantum noise provided by squeezed light. This work is an evaluation of the difficulties associated with operating such a detector in air and achieving a high degree of noise isolation.

Introduction

The project of characterizing homodyne detectors is an effort to investigate a potential improvement or replacement to the LIGO interferometer's signal readout method. The current LIGO setup makes use of a homodyne detection scheme involving DC readout (DCR). In DCR, a length offset is maintained between the interferometer's X and Y arms, leading to a static local oscillator (LO) field at the anti-symmetric (AS) port. A photodiode is placed at the AS port to monitor the power of the signal. As shown by Fritschel, et al., [1],

$$P_{AS} = \bar{P}_{AS} + 2Re(\bar{A}_{DC}(A_\sigma + \epsilon\bar{A}_{DC})^*), \tag{1}$$

where P_{AS} is the power at the dark port, A_{DC} is the LO field, A_σ is the field caused by the gravitational wave, ϵ is any noise present on the LO, and $\bar{P}_{AS} = \bar{A}_{DC}^2$. As can be seen in this equation, there is no variation in the relative phase between the gravitational wave (GW) and LO signals. It is fixed because the two signals co-propagate. However, the gravitational wave component of the power, the second term on the right-hand side, could be overshadowed by the average power of the LO field, $\bar{P}_{AS}$, and variations in LO noise can look deceptively akin to power variations due to GW.

In balanced homodyne readout (BHR), the LO is picked off from the carrier beam, and later interfered with the AS field on a beam splitter. The two output signals are detected with photodiodes and subtracted. The power difference in the photodiodes reveals the GW signal [1].

$$P_A - P_B = 2Re(e^{i\phi}\bar{A}_{LO}A_{\sigma}^*), \tag{2}$$

where $P_A - P_B$ is the difference in power between the two photodiodes, A_{LO} is the picked-off LO field, and ϕ is the phase difference between the GW and LO fields. The appearance of ϕ indicates that, in BHR, the LO phase must be known and controlled in order to detect a GW. However, the ϵ term has vanished in the subtraction, showing that all noise in the LO should cancel, in principle. Also, since the two photodiode signals have the same average power, $\bar{P}_{AS}$ is subtracted out, and no longer threatens to overshadow the GW signal in the readout.

BHR carries another advantage. It would allow for the implementation of squeezing, which would in turn allow for the measurement of sub-quantum noise. In order to measure sub-quantum noise, the squeezed shot noise must exceed the other most dominant noise source, which would be the electronics at the readout [1],

$$\frac{R}{\alpha F_{sqz}}\sqrt{2\epsilon P} \geq \sqrt{4k_BTR},$$

where R is the resistance of the transimpedance amplifier at the readout, α is the safety factor (margin between shot noise and electronics noise), F_{sqz} is the squeezing factor, and ϵ in the conversion factor between the signal power at the PDs, and the difference current. We can rearrange the equation to show,

$$\sqrt{R} \geq \alpha F_{sqz}\sqrt{\frac{2k_BT}{\epsilon P}}.$$

Thus, a larger resistor is favorable to measure sub-quantum noise. Currently, LIGO uses 400 Ω at the signal readout, which does not allow the inequality above. Due to the large output current in DCR, if R were to be increased, the output voltage would quickly escalate to levels unsupportable by detector electronics. In BHR, however, the current between the two photodiodes is subtracted before being read out, meaning that a large resistor can be used without the need to support high voltages.

In this study, we construct a BHD akin to the one discussed above, and evaluate its noise performance with the motivation of potentially implementing such a detector in the Advanced LIGO interferometer. In analyzing the noise performance, a consideration of the difficulty and practicality of the methods, as they would translate to full scale LIGO, must be kept in mind.

Intensity Stabilization

Prior to its construction, the BHD had unknown behavior with power noise. It was expected that, from Eq. 2, there would be a great deal of LO noise cancellation in the current subtraction between the two photodiodes. However, in order to optimize the noise at the BHD output, an intensity stabilization servo (ISS) was constructed to ensure a clean signal entering the BHD. A block diagram of the ISS can be seen in Fig. 1.

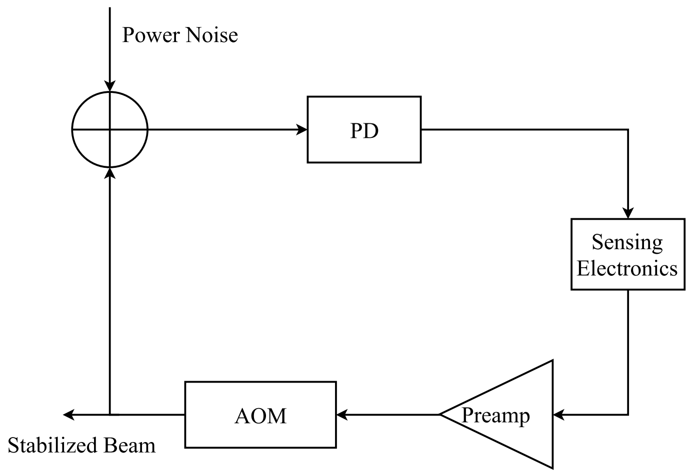

Figure 1: ISS block diagram.

The ISS was comprised of an acousto-optic modulator (AOM), a preamplifier, and a photodiode (PD) with filtering electronics. The AOM diverts power from the incoming beam by an amount that is proportional to its supplied voltage, and the preamp is set to apply a gain of 500. The sensing electronics are comprised of three RC circuit filters that implement a cutoff frequency of 500 Hz, with $\frac{1}{f^3}$ decay. The PD has a quantum efficiency of $\eta = 0.55$ which leads to an output current of $0.47\frac{A}{W}$. Additionally, at the PD readout, there is a 300 Ω resistor that effects a gain of $300\frac{V}{A}$, and a 10 nF capacitor creates a 53 kHz pole. In addition to the PD in the servo loop (ILPD), an out-of-loop PD (OLPD) was added as an external monitor that received the same same power as the ILPD via a 50/50 beamsplitter. A Bode plot of the ISS transfer function can be seen in Fig. 2.

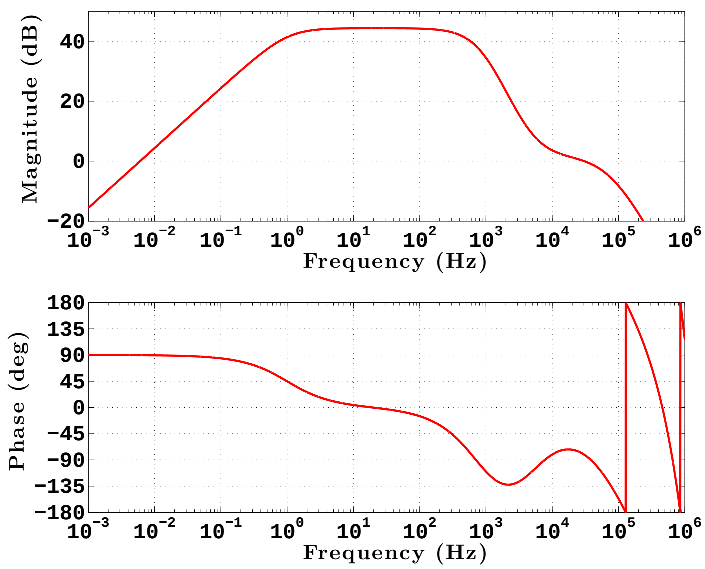

Figure 2: ISS open loop gain.

To model the expected noise suppression from the ISS, an ASD was collected at the output of the OLPD without the ISS providing control (free-running). This ASD was then used as an input to the closed loop transfer function of the ISS. Figure 3 shows the the free-running relative intensity noise (RIN), and the expected suppression from the ISS.

Amplitude spectra were then collected with the ISS running. Figure 4 shows several spectra of interest. The cyan curve shows the noise on the SR-785 spectrum analyzer with no input, and the magenta curve shows the noise present at the PD with no laser coming into the ISS. The green curve shows the noise observed at the OLPD output while the red curve shows the noise at the ILPD output. Finally, the black line is

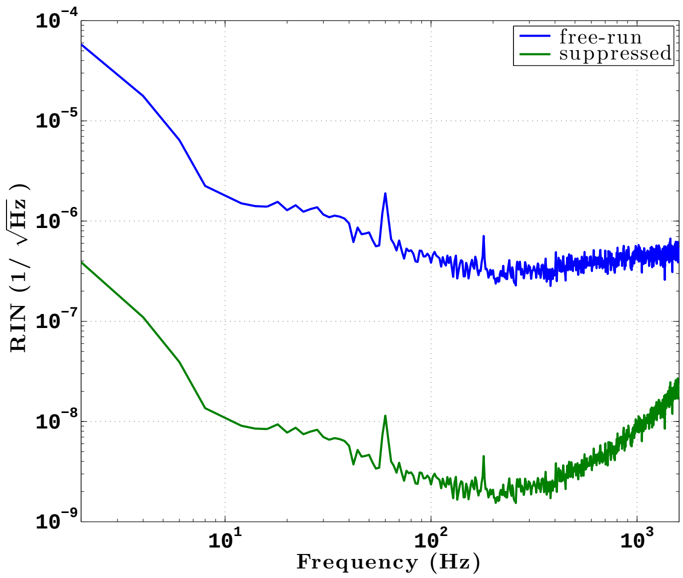

Figure 3: Modeled ISS noise suppression.

the shot noise corresponding to the 4.5 μW flowing through either of the PDs. Note that the ILPD shows suppression below the shot noise because the error signal in the ISS can be artificially suppressed. The OLPD floor sits a factor of $\sqrt{2}$ above the shot noise because the OLPD accounts for the currents in both of the PDs. This factor of $\sqrt{2}$ is expected, and indicates that the output of the ISS is shot noise limited. The analyzer noise and dark noise also descend below the shot noise around 70 Hz, and are not measurable with the laser on.

The BHD

The beam, stabilized by the ISS, enters the BHR arrangement. The setup involves four highly reflective mirrors (HR), a partially transmitting mirror, a piezo-controlled mirror, a non-polarizing 50/50 beam splitter and a photodiode electronics board, on which two photodiodes are wired for current subtraction (Fig. 5). The beam from the piezo-controlled mirror can be used as the local oscillator from Evans' equations, and the dashed line will be the signal field [1].

Noise analysis was performed with signal field blocked by a beam dump, which is akin to the current LIGO DCR scheme. After aligning the two LO signals to the photodiodes, their output voltages were read and spectra were collected. In principle, with the signal field blocked, all noise but the shot noise should be canceled in the current subtraction. Figure 6 shows the spectra of the incoming beam (OLPD), the

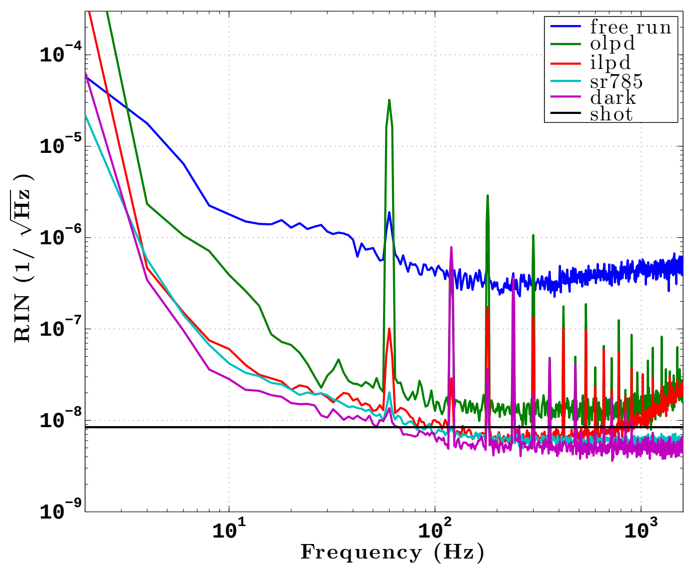

Figure 4: Measured ISS noise suppression.

difference current output (DC) and the shot noise floor.

Comparing the OLPD noise to the DC noise, it can be seen that the current subtraction in the PD circuit cancels noise quite well. The shelf at the lower frequencies can be attributed to room noise, such as air currents lightly forcing the mirrors, or dust particles drifting through a certain part of the beam. Notice that the large 60 Hz harmonics are greatly cancelled in the DC signal. In the higher frequencies, above roughly 2 kHz, the ISS offers little noise suppression, but there is no noticeable increase in DC noise as this suppression rolls off. This suggests that the ISS is unnecessary for power stabilization. So, the ISS was discarded for the rest of the experiment.

Although the BHR circuit seems to be successful in canceling large amounts of noise, the distribution shown in Figure 6 has some unexpected features. The DC noise is a factor of $\sqrt{2}$ higher than the shot noise ,and therefore a factor of $\sqrt{2}$ higher than expected. Also, there is a prominent noise peak at about 150 Hz, which was determined to be caused by vibrations in the table.

In order to isolate the BHD from noise sources in the room, we constructed a box of aluminum and foam to be placed over the entire detector setup, with a hole to allow the entrance of the beam from the NPRO (Fig. 7), which was measured to provide 20 dB of acoustic isolation. In addition, the BHD was elevated on silicon rubber feet in order to isolate it from vibrations in the table (Fig. 8).

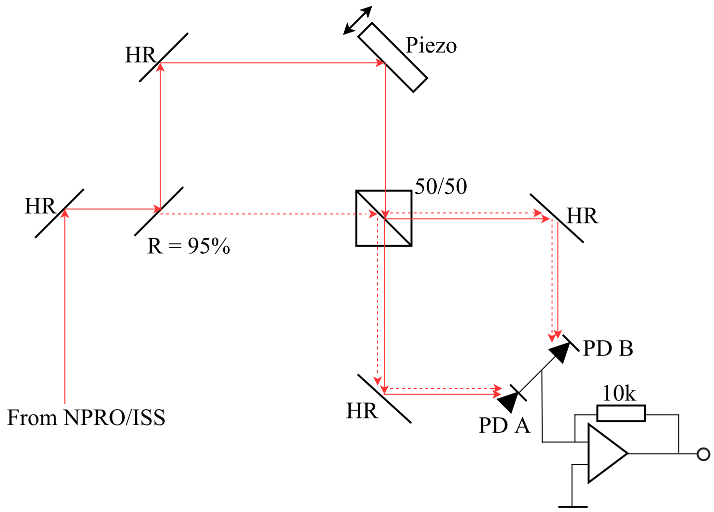

Figure 5: The homdyne detector setup.

Phase Noise and Amplitude Noise

As shown in Eq. 2, the implementation of the BHD requires controlling the homodyne phase, ϕ. Steinlechner, et al. show how the individual photodiodes vary with the homodyne phase [2].

$$V_A = \frac{e\eta_a R}{2h\nu}(P_{LO} + P_\sigma + 2\sqrt{P_{LO}P_\sigma}\cos\phi), \tag{3}$$

and

$$V_B = \frac{e\eta_B R}{2h\nu}(P_{LO} + P_\sigma - 2\sqrt{P_{LO}P_\sigma}\cos\phi), \tag{4}$$

where R represents the 100 Ω resistor over which each PD is read out. A graphical representation of V_A and V_B can be seen in Fig. 9.

To understand how the difference current voltage readout responds to phase noise, we can use an expression derived by Steinlechner, et al. [2].

$$\delta i_-^2 = 4P_{LO}\delta X^2_{-\phi,\sigma} + 4P_\sigma \delta X^2_{\phi,LO}, \tag{5}$$

where δi_- is the noise variance in the difference current, P_{LO} is the power in the local oscillator path, P_σ is the power in the signal path, ϕ is the phase between the two fields due to difference in length between the LO and signal paths, and $X_{\theta,A} = X_{1,A}\cos\theta + X_{2,A}\sin\theta$. It can be seen that noise in the LO field is scaled by the power in the signal field, and vice versa. If the BHR scheme is operated at $\phi = 90°$, then the noise variance in the difference current is dependent on noise in the phase quadrature of the two fields.

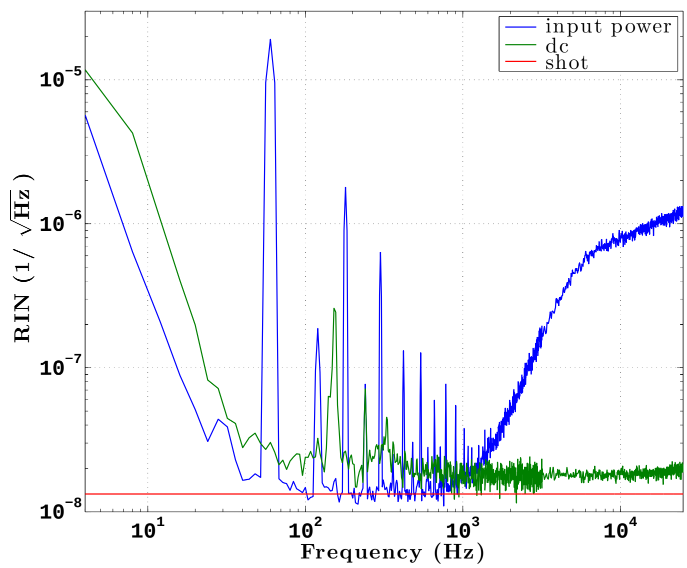

Figure 6: LO noise cancellation in the BHR difference current.

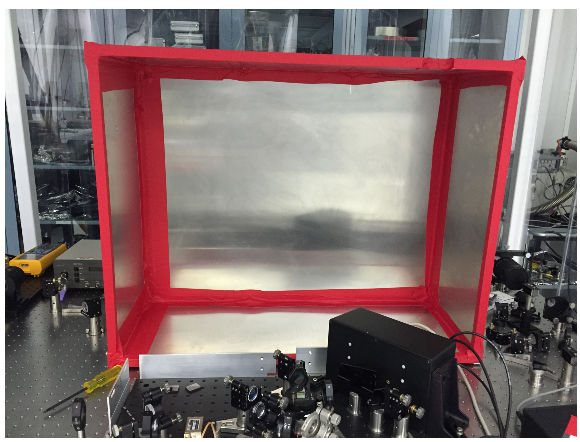

Figure 7: BHD acoustic box, providing 20 dB isolation.

$$\delta i_{-}^{2} = -4P_{LO}\delta X_{2,\sigma}^{2} + 4P_{\sigma}\delta X_{2,LO}^{2}. \tag{6}$$

Although the power in the signal field is much smaller than the power in the LO field (2 μW compared to 3 mW), with the injection of phase noise into the LO path by the piezo mirror, the second term in Eq. 6 dominates the noise variance.

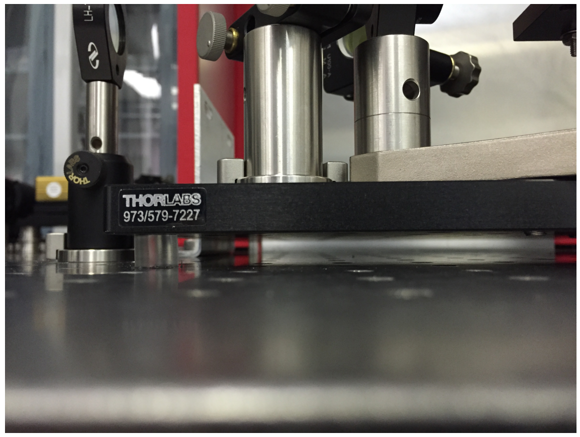

Figure 8: Silicon rubber feet for vibration isolation

$$\delta i_{-} \approx 2\sqrt{P_{\sigma}}\delta X_{2,LO}. \tag{7}$$

In Eq. 7, $\delta X_{2,LO}$ is a small change in phase in the LO path ($\delta\phi$), scaled by the LO field strength.

$$\delta i_{-} \approx 2\sqrt{P_{\sigma}}\sqrt{P_{LO}}\delta\phi\frac{\lambda e\eta}{hc}. \tag{8}$$

This expression includes a necessary conversion factor to achieve units of current, where η is the quantum efficiency of the photodiodes. Finally, an expression can be obtained that shows the phase noise response of the BHR difference voltage readout.

$$\frac{\delta V_{-}}{\delta\phi} \approx \frac{2\lambda e\eta R}{hc}\sqrt{P_{\sigma}P_{LO}}, \tag{9}$$

where R is the amplification resistance of the difference current, in this case 10 $k\Omega$. Figure 10 shows the theoretical phase noise transfer function, with and without an ND filter in the signal path, as well as measured curves.

Note that both of the theoretical curves were calculated for a $\phi = 90°$ homodyne phase. The power in the LO field was 3 mW, and an ND filter was used to attenuate the signal field power from 176 μW to 2 μW. Although there is a discrepancy between the theoretical transfer functions and the measured transfer functions in the phase quadrature ($\phi = 90°$), notice that the offset between theory and measurement goes unchanged after the application of the ND filter. A future goal is to obtain measurements over a larger range of frequencies, but this is, in practice, limited by the difficult task of controlling the homodyne phase while applying phase noise excitation. The slow drift away from the theory curves is possibly due to the homodyne phase drifting during the collection of data. There was an attempt to servo the piezo-controlled mirror using phase loop locking with RF modulation, but the RF component of the homodyne electronics did not perform as expected. Instead, the mirror was controlled

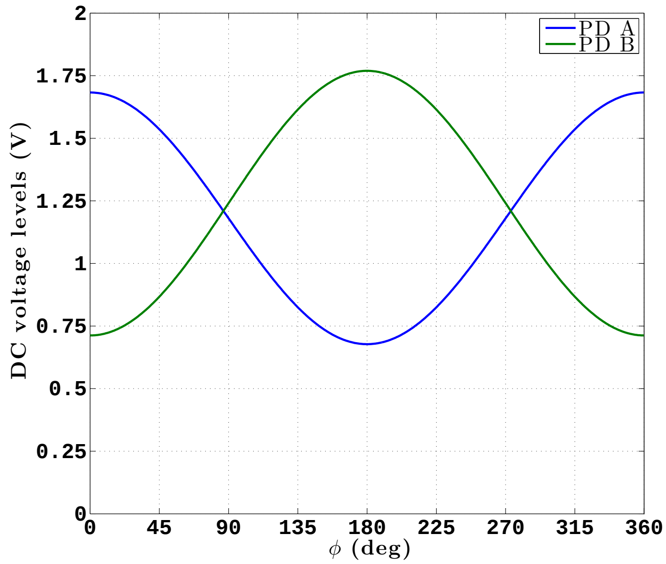

Figure 9: PD voltages as a function of homodyne phase, ϕ

by keeping the individual PD voltages as close as possible ($\phi \approx 90°$), or maximally different ($\phi \approx 0°$), (see Fig. 9)

If instead, $\phi = 0°$ was chosen as the operating point, Eq. 5 reduces to show a noise variance dependent on noise in the amplitude quadrature.

$$\delta i_-^2 = 4P_{LO}\delta X_{1,\sigma}^2 + 4P_\sigma \delta X_{1,LO}^2. \tag{10}$$

In principle, the output current while operating in the amplitude quadrature ($\phi = 0°$), is insensitive to phase noise in either field. Rather, Eq. 10 suggests that any noise observed in the output current while exciting phase noise must be attributed to amplitude noise. A measurement of the phase noise transfer function in the amplitude quadrature collected on July 28, 2015, the blue line in Fig. 10, showed the expected result. The magnitude sits roughly four decades below the curve in the phase quadrature, and the coherence is low, indicating that the difference voltage output is strongly independent of the phase noise input. However, a similar measurement collected two days later shows a response magnitude decades higher. It is possible that there is some undiscovered source of scattering that couples phase noise into the amplitude quadrature during the modulation.

Another surprise is the detector's response to amplitude noise. In principle, the difference current is insensitive to amplitude noise in the LO when operating in the phase quadrature ($\phi = 90°$), and maximally sensitive to amplitude noise in the LO when operating in the amplitude quadrature ($\phi = 0°$). However, in measuring the

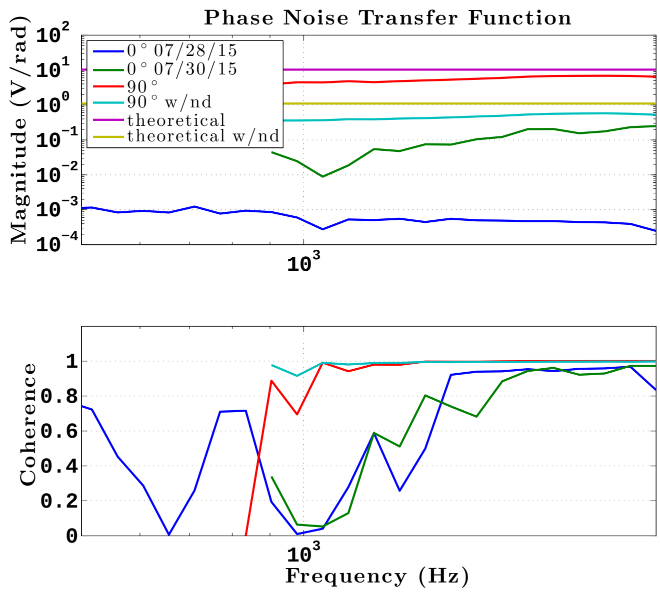

Figure 10: Phase noise transfer function of the BHD.

amplitude noise transfer function of the BHD (Fig. 11), these principles were not observed.

Looking at the two $\phi = 0°$ lines, we see that the ND filter provided the expected attentuation, as in the phase noise transfer function of Fig. 10. However, when the homodyne phase was adjusted to $\phi = 90°$, with the ND filter still in the signal path, there was no change in the sensitivity at the difference current output. There must be some sort of mechanism by which amplitude and phase noise are coupled in the detector. It is possible that not all of the reflected beams were caught, and the scattering causes amplitude noise responses when phase noise is injected into the detector, and vice versa.

Power Noise

To investigate the influence of power noise in the BHR scheme, we can look at the RIN transfer function associated with the difference current. As derived by Steinlechner, et al.[2],

$$i_A \propto \frac{1}{2}(P_{LO} + P_\sigma + 2\sqrt{P_{LO}}\sqrt{P_\sigma}\cos\phi) \tag{11}$$

$$i_B \propto \frac{1}{2}(P_{LO} + P_\sigma - 2\sqrt{P_{LO}}\sqrt{P_\sigma}\cos\phi), \tag{12}$$

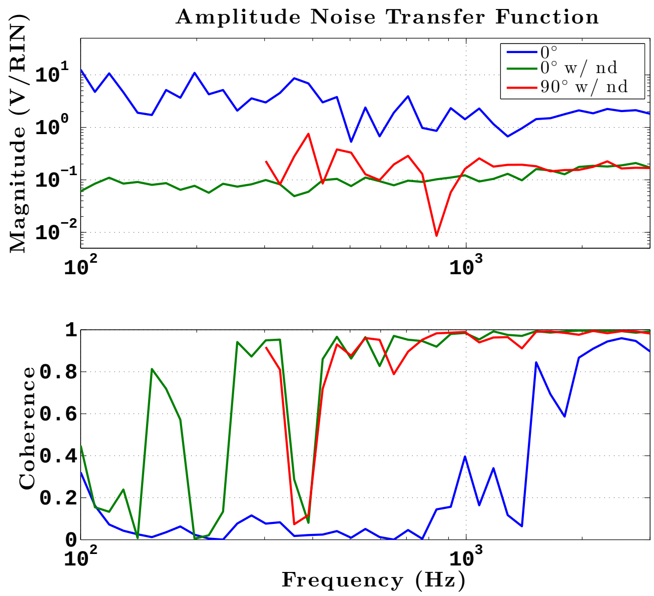

Figure 11: Amplitude noise transfer function of the BHD

or more exactly,

$$i_A = \frac{1}{2}(P_{LO} + P_\sigma + 2\sqrt{P_{LO}}\sqrt{P_\sigma}\cos\phi)\frac{\eta_A e}{h\nu} \tag{13}$$

$$i_B = \frac{1}{2}(P_{LO} + P_\sigma - 2\sqrt{P_{LO}}\sqrt{P_\sigma}\cos\phi)\frac{\eta_B e}{h\nu}. \tag{14}$$

Then the difference current is

$$i_- = i_B - i_A, \tag{15}$$

and

$$RIN_{i_-} = \frac{2i_-}{i_A + i_B}. \tag{16}$$

To predict the ASD associated with the free-running power noise, we can simply multiply the measured noise by the RIN transfer function and convert to $\frac{V}{\sqrt{Hz}}$.

$$ASD = RIN_{free}RIN_{i_-}iR. \tag{17}$$

The unsuppressed power noise and the predicted noise cancellation at $\phi = 90°$ can be seen in Fig. 12 as the blue curve and green curve, respectively.

The BHR scheme is very good at cancelling power noise, as evidenced by the fact that the 90° homodyne phase curve sits well beneath the shot noise floor. The frequency

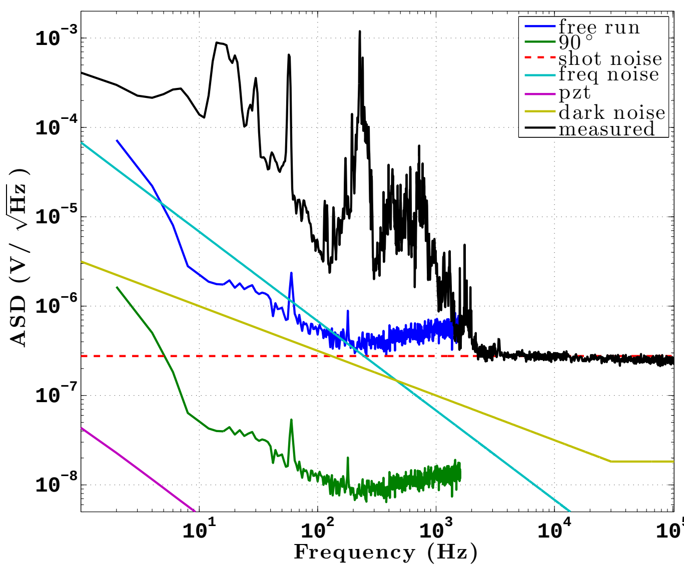

Figure 12: BHR noise budget with ND filter.

noise curve is extrapolated from a noise coupling measurement of $6.8 \times 10^{-6}\ \frac{V}{Hz}$ taken when the NRPO frequency was modulated at 8 kHz, and combined with the laser's noise curve, which is roughly $\frac{10^4}{f}\ \frac{Hz}{\sqrt{Hz}}$. In order to filter electronics noise between the the piezo mirror driver and the analog-to-digital interface with the computer system, a 1 $M\Omega$ resistor was added to the output of the piezo driver. The piezo mirror has a capacitance of 450 nF, which, with the resistor, creates a pole at 0.3 Hz. The spectra of the piezo driver and digital-to-analog (D2A) electronics were observed. The driver itself had s flat noise curve of 500 $\frac{nV}{\sqrt{Hz}}$. The D2A card dominates the electronics noise with a flat curve of 2 $\frac{\mu V}{\sqrt{Hz}}$ after the gain of the piezo driver. The D2A curve was filtered with the 0.3 Hz piezo pole, and passed through the phase noise transfer function from Fig. 10 to yield the magenta curve in Fig. 12. With no laser coming into the BHR scheme, that is, no LO and no signal fields, an ASD similar to the yellow curve was observed.

The black curve in Fig. 12 is the current standing of the noise performance of the BHR scheme. The ultimate goal, of course, is to reach the shot noise floor at all frequencies. The peak around 30 Hz is likely caused by the laboratory air conditioning, so perhaps there is more work to be done in isolating the detector. By comparing the blue and black curves, it is evident that other noise sources have been introduced in the BHR setup. A likely culprit is scattering off of some of the optics in use that has, thus far, gone undetected, or acoustic disturbances sneaking through the isolation box.

Conclusions

By looking at the black and red curves in Fig. 12, we can draw two important conclusions about the balanced homodyne detector. While operating in the phase quadrature, the BHD hits shot noise at frequencies in excess of 1 kHz. Ideally, the spectrum of the difference current would be shot noise at all frequencies, but this is not the case in practice. At lower frequencies, it appears that the detector is dominated by acoustic noise. The detector was isolated with silicon rubber feet and an acoustic box, but this may not be enough. Operating this detector in air is difficult.

References

[1] P. Fritschel, M. Evans, V. Frolov. *Balanced Homodyne Readout for Quantum Limited Gravitational Wave Detectors*. LIGO Laboratory, Massachusetts Institute of Technology, Cambridge. 2013.

[2] Steinlechner, et al. 'Local-Oscillator Noise Coupling in Balanced Homodyne Readout for Advanced Gravitational Wave Detectors'. SUPA, School of Physics and Astronomy, The University of Glasgow, Glasgow, UK.